Principles of Nonequal Channel Angular Pressing

Arman Hasani
László S. Tóth
Benoît Beausir

Laboratoire de Physique et Mécanique des Matériaux,
Université Paul Verlaine de Metz,
Ile du Saulcy,
57045 Metz, France

A variant of the equal channel angular pressing (ECAP) process is examined in this paper where the channels are of rectangular shape with different thicknesses while the widths of the channels are the same. The process is named nonequal channel angular pressing and it is similar to the earlier introduced dissimilar channel angular pressing (DCAP) process. In DCAP, however, the diameters are near values, with the exit channel being slightly larger, while in NECAP, the exit channel is much smaller attributing several advantages to nonequal channel angular pressing (NECAP) with respect to ECAP. In this work an analysis is performed to determine the strain mode in a 90 deg NECAP die. A new flow line function is also presented to better describe the deformation field. The proposed flow line function is validated using finite element simulations. A comparison is made between ECAP and NECAP. Finally, texture predictions are presented for NECAP of fcc polycrystals. The advantages of this severe plastic deformation process are the following: (i) significantly larger strains can be obtained in one pass with respect to the classical ECAP process, (ii) grains become more elongated that enhances their fragmentation, and (iii) large hydrostatic stresses develop that improve the stability of the deformation process for difficult-to-work materials. The results obtained concerning the deformation field are also applicable in the machining process for the plastic strains that imparted into the chips. [DOI: 10.1115/1.4001261]

Keywords: ECAP, DCAP, simple shear, flow line modeling, texture

1 Introduction

Equal channel angular pressing (ECAP) is a severe plastic deformation process that was invented by Segal [1–3]. It has received real attention only since the beginning of the 1990s when it was shown that this severe plastic deformation (SPD) process can produce bulk materials with very fine grain sizes. The ECAP process involves imposing very large plastic strains on a work piece without changing the cross-sectional dimensions, which ultimately refines the grain size down to ~200 nm with improved mechanical and physical properties, see the review of Valiev and Langdon [4]. Its main principle is that a bulk sample is extruded through two channels with equal cross sections that are connected to each other by an angle between 60 deg and 135 deg. The work piece is extruded with the help of a piston. As there is no change in the cross section, the sample can be re-introduced into the inlet channel and can be extruded several times. Difficult-to-work materials can be also extruded with the help of a back pressure that is exerted by a second piston in the outgoing channel [5].

In the present work, such angular extrusion is considered in which there is no rounding of the corners at the intersection of the channels. A modification of the ECAP process was first examined by Lee [6] in which the thicknesses of the two channels were considered to be different (NECAP). Lee [6] carried out an upper-bound analysis to estimate the pressing stress and obtained also a formula for the shear strain in one pass:

$$\gamma = \cot\alpha + \cot\beta \tag{1}$$

where α and β are the angles of the intersection plane with the inlet and outlet channels, respectively. Equation (1) can be rewritten for a 90 deg die as

$$\gamma = \frac{p}{c} + \frac{c}{p} \tag{2}$$

where p and c are the thicknesses of the inlet and exit channels, respectively. DCAP was then applied in the continuous confined strip shearing (C2S2) process of metal sheets that aims to develop good textures in aluminum to improve formability [7–11]. These DCAP applications were limited to a 120 deg die and relatively small differences in the diameters of the channels; the ratio K of the inlet and exit channel diameters was only $K=t_0/t_f=0.935$. Note that the exiting sheet had larger thickness. Actually, it is also the case for the chip formation in machining where the chip diameter is always larger than the depth of cutting. Lee et al. [8] also proposed a formula for the total strain in DCAP, which is the following for one pass:

$$\gamma = 2K^2 \cot\frac{\Phi}{2} \tag{3}$$

where Φ is the die angle. Using again p and c for the channel diameters, Eq. (3) takes the following form for a 90 deg die:

$$\gamma = 2\left(\frac{p}{c}\right)^2 \tag{4}$$

Obviously, Eq. (4) is different from Eq. (2). The difference is large; for example, for the typical ratio of $p/c=0.935$ used in DCAP, Eq. (3) gives $\gamma=1.748$, while from Eq. (2), we get $\gamma=2.005$. The latter value is almost the same as the value of $\gamma=2$ known for a 90 deg ECAP die [12] while the first is significantly smaller. It is important to use the right formula for the estimation of the strain in DCAP or NECAP, which will be one of the objectives of the present work. The differences come from the fact that the deformation mode in ECAP is still not commonly understood or agreed in the scientific community. For example, Eq. (4) is obtained in Ref. [8] by assuming that simple shear takes place *parallel* to the exit channel. Another assumption was made in Ref. [13] where it was taken to be *perpendicular* to the intersection plane of the channels. However, other analyses have shown that the shear is actually parallel to the intersection plane of the chan-

Contributed by the Materials Division of ASME for publication in the JOURNAL OF ENGINEERING MATERIALS AND TECHNOLOGY. Manuscript received January 27, 2009; final manuscript received February 1, 2010; published online June 15, 2010. Assoc. Editor: Georges Cailletaud.

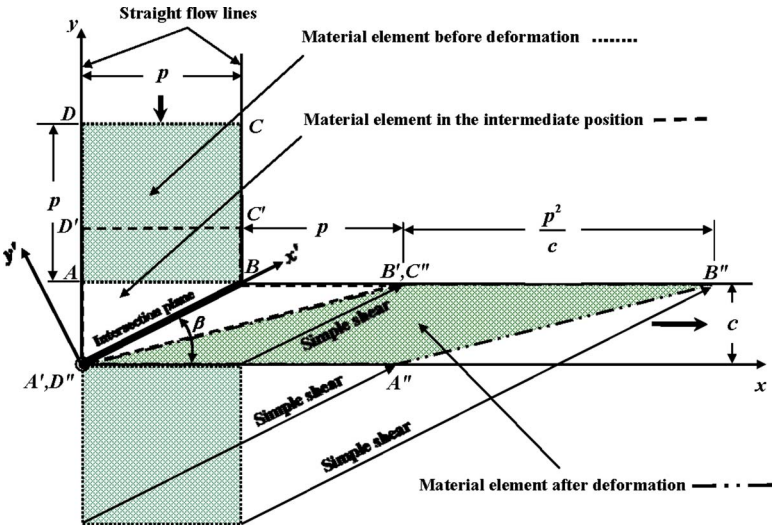

Fig. 1 Ideal geometry of the NECAP process

nels in ECAP [12,14,15]. It will be shown in the present work that it is the case not only in ECAP but also in the more general angular extrusion case, i.e., in NECAP and that Eq. (2) is the right formula for the total strain.

Although the ECAP process is very effective in refining the microstructure, several passes are required to reach the desired properties. This noncontinuous aspect makes the process difficult to introduce into technical applications. Although there exist several propositions to make the process continuous [16–19], all of them have certain disadvantages (usually too much heating of the work piece during the process). It is therefore interesting to enhance the grain refinement in one pass in order to reduce the total number of passes until the desired fine microstructure is achieved. One way to increase the strain in one pass is to decrease the cross section of the outgoing channel (NECAP). The principles of such angular extrusion process are examined in the present work.

There is a great similarity between the ECAP process and orthogonal cutting (machining). However, there is a subtle difference too; in orthogonal cutting, the thickness of the chip is not equal to the depth of cut. The modified process may have a similar methodology of experimentation with the only difference that the thickness of the outlet channel is smaller than the inlet channel. The process could give the additional benefit of obtaining strips with all the attributes that a normal ECAP processed material may have. In the present analysis, the amount of strain imparted per pass has been estimated, and is shown to be significantly larger than in normal ECAP. In this respect and in order to describe the material flow during orthogonal cutting process, an inequality in the size of entrance and exit channels of ECAP should be imposed.

The objective of this paper is to provide a theoretical foundation to the process. An analytical model of deformation for a 90 deg NECAP die based on a flow line pathway is presented. This flow line function was inspired from the one presented for 90 deg ECAP [15]. The modeling by the classical discontinuous simple shear model is also analyzed and discussed. The obtained results are compared with previous results in 90 deg ECAP [2,15] and also validated by finite element simulations.

2 Theoretical Foundation

The geometry of the process for a 90 deg die is presented in Fig. 1. The diameter of the entry channel is p and the exit channel is c. A practical value of the ratio of p/c is 2.0, which permits to reinsert the extruded specimen—after cutting it into two and stacking the two parts—just like in the accumulated roll bonding process [20]. Therefore, this case will be paid a special attention in the following.

In the ECAP process, the deformation can be idealized as a simple shear process that takes place in the intersection plane of the two channels (when the two channels are connected without any rounding, i.e., for sharp corners). This fundamental nature of the ECAP deformation is also valid in the present "NECAP" case, however, with a larger shear strain. In this section, the shape change of a material element is examined in order to verify the strain mode within the die.

2.1 Shape Change. We consider two straight flow lines that are initially separated from each other by a distance of p and consider a material element in square shape, which is defined by the points A-B-C-D, see Fig. 1. As this element flows through the plastic zone (which is considered to be very narrow), it changes to a parallelogram shape (defined by A''-B''-C''-D''). In order to set up suitable geometrical relations, we consider an intermediate position when the A point of the material element arrives to the corner of the die and the deformed shape is defined by the A'-B'-C'-D' points (dashed lines in Fig. 1).

The entering material flow velocity (vertical channel) is v_p and the exit is v_c (horizontal channel). In the intermediate position, the displacements of the A, C, and D points are equal to c and B changes its position to B'. The distance BB' can be obtained as follows. The time required to reach the intermediate position is

$$t_1 = \frac{c}{v_p} = \frac{BB'}{v_c} \tag{5}$$

Using now the continuity relation

$$pv_p = cv_c \tag{6}$$

we obtain $BB' = p$, which is indicated in Fig. 1. Now the element is further pushed to pass entirely the plastic zone. So D' is displaced by p to reach its corner position D''. The time needed for this is equal to the time between the A and A' positions:

$$t_2 = \frac{p}{v_p} = \frac{A'A''}{v_c} \tag{7}$$

Using again the continuity relation, we obtain

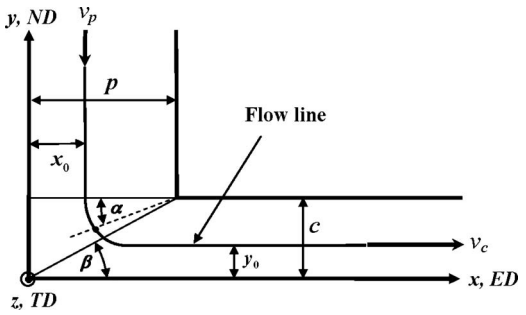

Fig. 2 Geometrical parameters for the flow line description of NECAP

$$A'A'' = \frac{p^2}{c} \tag{8}$$

The same distance must be between C'' and B''. Concerning the distance between B and C'', by using the time needed to get the C' point into C'', which it is equal to p, one can readily show (in two steps) that C'' is the same as B' (Fig. 1).

2.2 Simple Shear Model. The simple shear model that was originally proposed for the ECAP deformation mode by Segal [12] can be also adopted for the NECAP deformation. Figure 1 shows how an initially square shaped material element can be sheared to obtain the deformed shape that fits into the outgoing channel. The plane of shear is the intersection plane between the two channels in the negative direction when a reference frame x'-y' is fixed to it, see Fig. 1. In this figure, the same square element is shown below the shear plane and then sheared as the arrows show it. The amount of shear can be readily calculated using the geometry of the simple shear process:

$$\gamma = \frac{p}{c} + \frac{c}{p} \tag{9}$$

Note that this formula is the same as Eq. (2) above obtained by Lee [6]. It gives $\gamma=2$ for equal channel extrusion, when $p=c$. For the case of $p/c=2$, the shear strain is $\gamma=2.5$.

It is important to verify that the simple shear mode presented in Fig. 2 leads to the same deformed shape of an initial square than the one obtained by the kinematical technique above (see Fig. 1). For this purpose, it is sufficient to calculate the dimensions of the parallelogram shown in Fig. 1, from the displacement field that corresponds to the simple shear given by Eq. (9) and acting on the intersection plane of the two channels. Indeed, the dimensions of the parallelogram can be readily calculated and found to be identical to the dimensions of the parallelogram obtained in Sec. 2.1 above. This is a direct proof that the deformation process in NECAP is simple shear along the intersection plane of the channels, just like in ECAP.

It is useful to express the simple shear deformation mode in the x-y-z reference system that is fixed to the die (Fig. 1). The velocity gradient in the x'-y'-z' reference system is

$$\underline{\underline{L}}' = -\begin{pmatrix} 0 & \dot{\gamma} & 0 \\ 0 & 0 & 0 \\ 0 & 0 & 0 \end{pmatrix}_{x',y',z'} \tag{10}$$

where $\dot{\gamma}$ is positive. The transformation matrix is

$$T = \begin{pmatrix} \cos\beta & -\sin\beta & 0 \\ \sin\beta & \cos\beta & 0 \\ 0 & 0 & 1 \end{pmatrix} \tag{11}$$

where the β angle is defined by $\beta=\arctan(c/p)$. Using the transformation formula $\underline{\underline{L}}=\underline{\underline{T}}\,\underline{\underline{L}}'\,\underline{\underline{T}}^t$, we obtain

$$\underline{\underline{L}} = \dot{\gamma}\begin{pmatrix} \sin\beta\cos\beta & -\cos^2\beta & 0 \\ \sin^2\beta & -\sin\beta\cos\beta & 0 \\ 0 & 0 & 0 \end{pmatrix}_{x,y,z} \tag{12}$$

The strain rate tensor is the symmetric part of $\underline{\underline{L}}$:

$$\underline{\underline{\dot{\varepsilon}}} = -\frac{\dot{\gamma}}{2}\begin{pmatrix} -\sin 2\beta & \cos 2\beta & 0 \\ \cos 2\beta & \sin 2\beta & 0 \\ 0 & 0 & 0 \end{pmatrix}_{x,y,z} \tag{13}$$

$\underline{\underline{L}}$ can be directly used in a polycrystal model in order to calculate the texture development during the NECAP process according to the simple shear model. Note that $\dot{\gamma}$ is theoretically infinite if the shear zone is really a single plane. However, in experiments and in finite element modeling, it was found that the shear zone has a finite thickness and the shear rate can be approximated by [21] $\dot{\gamma}=-v_{0x'}/h$, where h is the half-thickness of the shear zone and $v_{0x'}$ is the x' component of the input velocity.

3 Deformation Analysis Using an Analytic Flow Function

While the simple shear model is a good approximation of the deformation process in a NECAP die, a more general description is also proposed here, which is based on the flow line model that was introduced in Ref. [15]. The following analytical trajectory function is proposed to describe the shape of a flow line:

$$f = \left(1 - \frac{x}{p}\right)^n + \left(1 - \frac{y}{c}\right)^n = \left(1 - \frac{x_0}{p}\right)^n \tag{14}$$

In this expression, x_0 defines the incoming position of the flow line (Fig. 2) and n is a parameter affecting the shape of the flow line in the deformation zone. Note that the origin of the coordinate system is fixed at the lower left corner of the die in Fig. 2 and that the validity of the function is restricted to $0\le x\le p$, $0\le y\le c$. This function only differs from the ECAP 90 deg flow function [15] that here p and c can be different. In the particular case when p and c are equal, Eq. (14) becomes the same as the ECAP 90 deg flow function. The proposed function satisfies the boundary conditions imposed in the test concerning the direction of the flow at the entering and leaving positions of the corner region where plastic deformation is expected to take place. At these positions, which are defined by $x=x_0$ and $y=y_0$, respectively, the flow lines are parallel to the local velocity of the material. The n parameter defines the possible shapes of the flow lines: For $n=2$, the flow line is circular and by increasing n, the sharpness of the flow line increases. For the limiting case $n\to\infty$, the flow lines become connected straight lines. Actually, the flow lines used in Sec. 2 correspond to this limiting case.

It is known from fluid mechanics that in the case of incompressibility, an admissible velocity field can be defined from the trajectory function f as follows [22]:

$$v_x = \lambda\frac{\partial f}{\partial y}, \quad v_y = -\lambda\frac{\partial f}{\partial x} \tag{15}$$

This velocity field is tangent to the flow trajectory. $\partial f/\partial y$ and $\partial f/\partial x$ describe the variations of the velocity imposed by the geometry of the process and the λ parameter is introduced to scale the tangent vector to the material velocity. λ can be determined by the incoming velocity v_p, and one obtains

$$\lambda = -\frac{pv_p}{n}\left(1 - \frac{x_0}{p}\right)^{-n} \tag{16}$$

In this way, the velocity field is given by

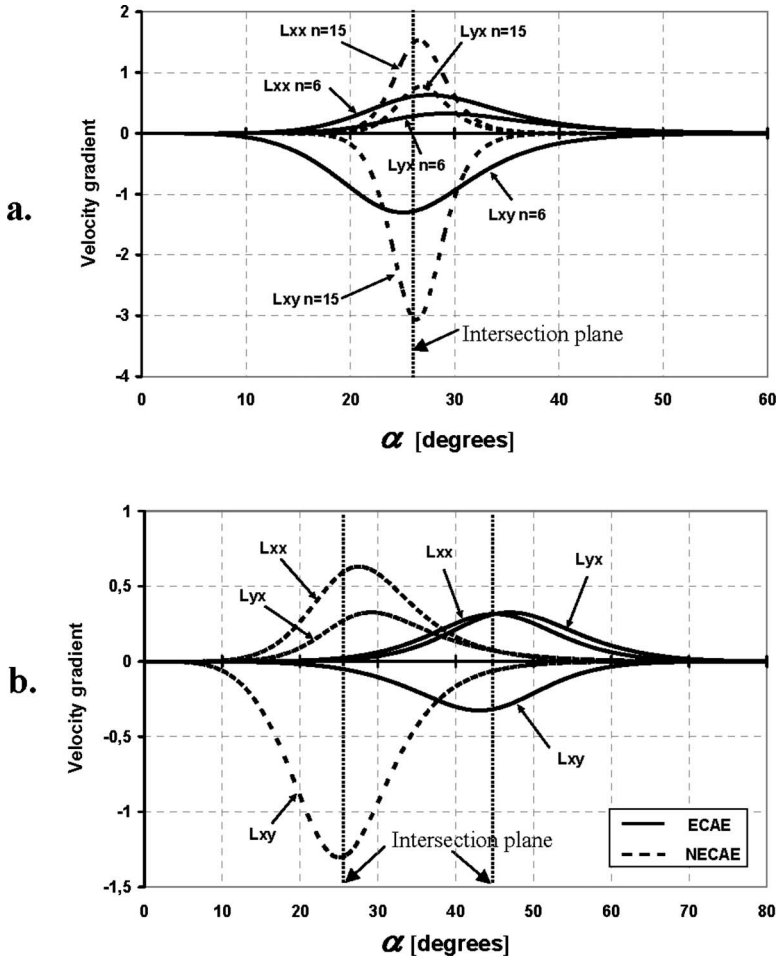

Fig. 3 Variations of the nonzero components of the velocity gradient as a function of the angular position along the flow line for $p/c=2$ in a 90 deg die. (*a*) Comparison for two values of the n parameter. (*b*) Comparison between ECAP and NECAP for $n=6$.

$$v_x = \frac{pv_p}{c}\left(1-\frac{y}{c}\right)^{n-1}\left(1-\frac{x_0}{p}\right)^{1-n}, \quad v_y = -v_p\left(1-\frac{x}{p}\right)^{n-1}\left(1-\frac{x_0}{p}\right)^{1-n} \tag{17}$$

The velocity gradient field can be obtained by partial derivation of the velocity field (Eq. (17)):

$$L_{xx} = \frac{\partial v_x}{\partial x} = \frac{v_p}{(p-x_0)}(n-1)\left(\frac{c}{p}\right)^{n-2}\left(\frac{c-y}{p-x}\right)^{n-1}\left(\left(\frac{c}{p}\right)^n + \left(\frac{c-y}{p-x}\right)^n\right)^{2/n-2}$$

$$L_{yy} = \frac{\partial v_y}{\partial y} = -L_{xx}$$

$$L_{xy} = \frac{\partial v_x}{\partial y} = -L_{xx}\frac{p-x}{c-y}$$

$$L_{yx} = \frac{\partial v_y}{\partial x} = L_{xx}\frac{c-y}{p-x} \tag{18}$$

The strain rate tensor is the symmetric part of $\boldsymbol{L}$, and it can be readily constructed from Eq. (18). The von Mises equivalent strain rate can be also obtained analytically:

$$\bar{\dot{\varepsilon}} = \frac{2}{\sqrt{3}}L_{xx}\sqrt{1+\frac{1}{4}\left(\frac{c-y}{p-x}-\frac{p-x}{c-y}\right)^2} \tag{19}$$

As can be seen, the above formulas describe a continuously varying strain field. It is useful to visualize the strain rate field along a flow line. For this purpose, the x and y coordinates can be replaced by one single parameter, the angular position α along the flow line, see its definition in Fig. 2. This angle is given by the relation $\tan\alpha=(c-y)/(p-x)$, which appears directly in the above formulas (Eqs. (18) and (19)). Figure 3 displays the variations in the velocity gradient field along the flow line for $p/c=2$ and for two values of the n parameter; $n=6$ and $n=15$, as a function of the α coordinate.

As can be seen in Fig. 3, there is tension in the x direction (L_{xx} is positive), there is compression along the y axis (L_{yy} is negative), and there are shears along the x and y planes with different amounts. The shear on the x plane (L_{yx}) is positive in the y direction while the shear on the y plane (L_{xy}) is negative in the x direction. The magnitudes of the velocity gradient components vary with n; by increasing the n value, the strain rate increases. At the same time, the deformation zone decreases (see Fig. 3(*a*)). For a given n value, the largest strain component is a shear component: the L_{xy}. One can see also in Fig. 3(*a*) that the positions of the maxima of the individual velocity gradient components do not coincide with the position of the intersection plane of the two channels. The deviation decreases, however, as the n value is in-

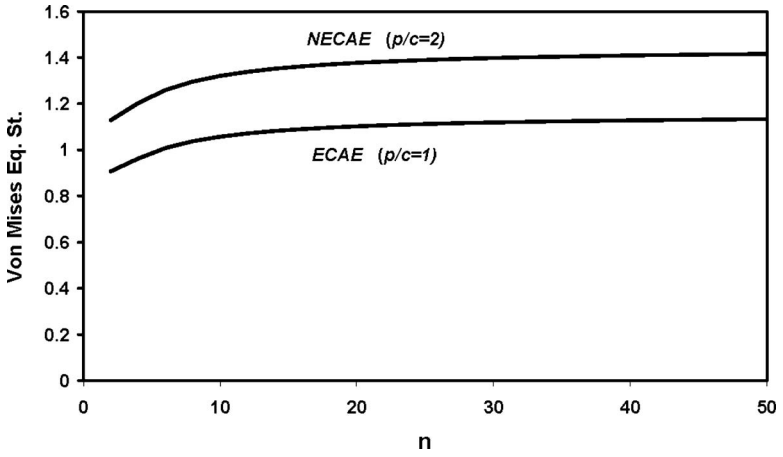

Fig. 4 Dependence of the accumulated equivalent von Mises strain on the *n* parameter for ECAP–90 deg ($p/c=1$) and NECAP-90 deg ($p/c=2$) in one pass

creased from $n=6$ to $n=15$. Actually, for $n\to\infty$, the flow line model coincides with the simple shear model, and in that case, the positions of the maximum values all agree with the position of the intersection plane (ideally, there is strain only in the intersection plane).

Figure 3(*b*) shows a comparison between the velocity gradient components between the ECAP and NECAP ($p/c=2$) deformation mode for the same n parameter ($n=6$) and for 90 deg dies. One can see that the characteristics of the deformation process in NECAP are quite similar to the ECAP deformation mode with the difference that the L_{xy} component becomes the major one in NECAP. The deformation zones are also displaced because the inclination of the intersection plane is different: It is at $\alpha=26.5$ deg in NECAP (for $p/c=2$), while it is at $\alpha=45$ deg in ECAP.

The von Mises equivalent strain in one pass is displayed in Fig. 4 as a function of the n parameter for both ECAP and NECAP ($p/c=2$). The curves begin at the smallest physically realistic value of the n parameter; $n=2$. The variations in ECAP were already discussed in Ref. [15]. As it is expected, the strain in NECAP is significantly larger, by about 25%. The limiting maximum values are $\bar{\varepsilon}=1.15$ ($\gamma=2$) and $\bar{\varepsilon}=1.44$ ($\gamma=2.5$), for ECAP and NECAP, respectively.

4 Crystallographic Texture

As it was shown in Ref. [15], the ideal orientations of ECAP can be readily obtained from the ideal orientations of simple shear. Such an analysis is pertinent in this work too, as it was shown above that the NECAP process ideally can be also approximated by simple shear. The top part of Fig. 5 displays the ideal orientations that belong to the simple shear process for fcc crystals in the x'-y'-z' reference frame, that is, on the intersection plane of the channels. (For the definitions of the ideal orientations, see Ref. [15].) Only the $\phi_2=0$ deg and $\phi_2=45$ deg sections of the whole Euler orientation space are shown here as they contain all major components of the textures that can develop in simple shear. For a 90 deg ECAP die, the very same ideal components are simply shifted by 45 deg when they are expressed in the x-y-z ECAP reference frame. For the NECAP case, when $p/c=2$, this shift is reduced to only 26.5 deg.

In the following, texture simulation results will be presented using the self-consistent polycrystal model together with the simple shear as well as the flow line models. Similar modeling approaches were proven to be successful for all material classes and for different die angles. For a comprehensive presentation of the state of the art in modeling of texture development in ECAP, see the recent review by Beyerlein and Tóth [23].

Texture development was calculated for a polycrystal containing 2000 randomly selected grain orientations. The self-consistent viscoplastic polycrystal model of Molinari and Toth [24] was used in its finite-element-tuned version [24] using the 12 $\{111\}\langle 110\rangle$ slip systems of fcc crystals. The strain rate sensitivity index was $m=0.05$ and the effect of hardening was neglected. The simulation results are shown in orientation distribution function (ODF) form in Fig. 5 as well as in $\{111\}$ pole figures in Fig. 6.

Texture simulations were done for ECAP as well as for NECAP ($p/c=2$), for 90 deg die, using both the simple shear and flow line models with $n=6$. The ECAP case was only repeated here for a possible comparison between ECAP and NECAP. As can be seen in Fig. 5, the textures that predicted by either the ECAP or NECAP processes are strong near the ideal components. The agreement of the positions of the local maxima in the ODF with the ideal orientations is better with the simple shear model. The use of the flow line model produces two effects.

1. The textures are significantly stronger compared with the simple shear model (see the maximum intensity values indicated in Fig. 5).
2. The texture components are rotated more from the ideal positions, in the opposite direction, and with angles depending on the texture component.

These rotations are well illustrated in the pole figures in Fig. 6 that show the entire texture (the ODF is presented in only two sections in Fig. 5). This latter effect was already discussed in Refs. [15,25] and is in agreement with experiments in ECAP. The other effect, the strengthening of the texture with the flow line model, has not been identified before. It is certainly due to the deviations of the strain mode from simple shear in the case of the flow line approach.

When the texture strengths obtained for ECAP and NECAP are compared, interestingly, relatively small differences exist in the ODF (see the values in Fig. 5). For NECAP, the texture is just slightly stronger although the plastic strain is about 25% more. More differences can be identified in the pole figure presentations of the textures (Fig. 6) where it is clear that the texture is the strongest in the NECAP case when the flow line model is used. The relatively small differences in the texture strength indicate that the texture is already well developed (meaning that the grains have already reached the vicinity of the ideal orientations) for a shear strain of $\gamma=2$, which is the strain in the classical 90 deg ECAP process. An additional 25% strain does not increase the overall texture strength significantly (due to the small intensity of the velocity field near to the ideal orientations), although some

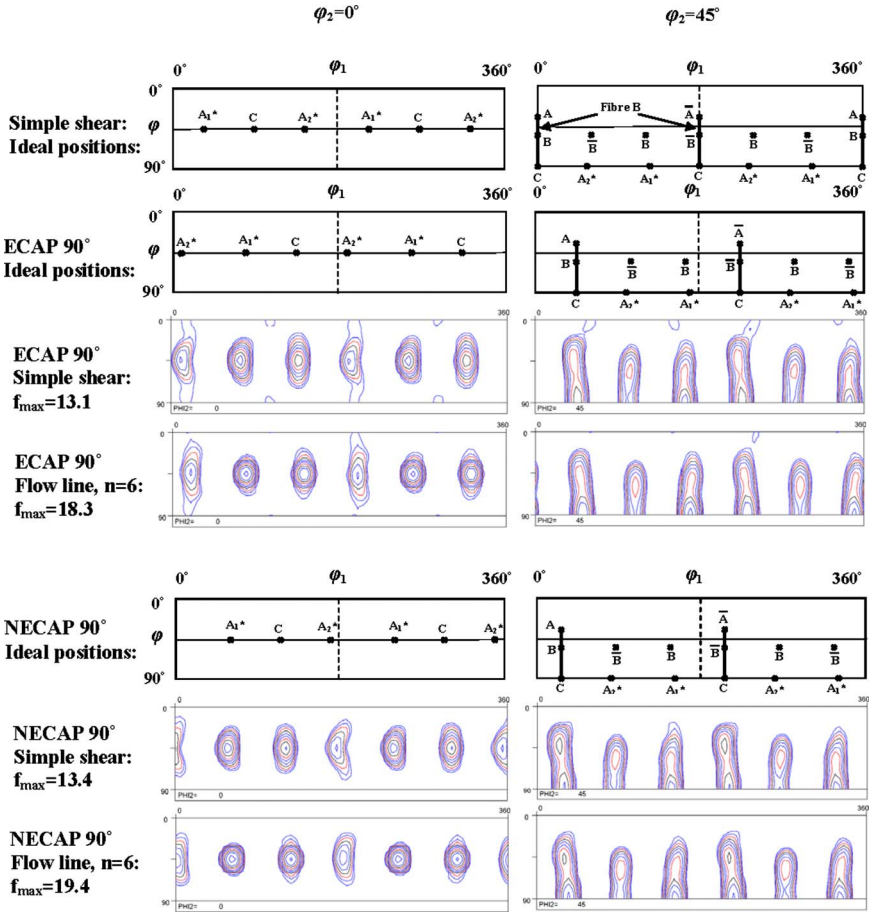

Fig. 5 The ideal orientations of simple shear and ECAP deformations as well as the textures that develop in one pass shown in two sections of the ODF. For NECAP, $p/c=2$. Isovalues in the ODFs: 0.7, 1, 1.4, 2, 2.8, 4, 5.6, 8, 11, and 16.

components strengthen more than the others (these are the $A/\bar{A}$ and $A1^*$ and $A2^*$ components). Detailed experimental measurements are needed to confirm/infirm the presented theoretical predictions.

5 Flow Lines From Finite Element Simulations

Finite element simulations were carried out to obtain trajectories during the NECAP extrusion process. Plane strain hypothesis was considered in order to simplify the analysis. The simulations were carried out with the help of the finite element ABAQUS explicit code. Four node bilinear plane strain quadrilateral elements with reduced integration were used for the workpiece. The width of the workpiece was 10 mm and the length 35 mm. The element size was 250×250 μm^2, which correspond to a number of 40 $\times140$ elements. It is sufficiently small because already a size of 1×1 mm^2 was found to be small enough to represent the local behavior of the workpiece [26]. In order to focus only on the geometrical parameter effects, no strain hardening and no strain rate effects were taken into account in the computation. The material is assumed to exhibit an isotropic elastic perfectly plastic behavior. The elastic material properties of the specimen are those of the pure aluminum with Young modulus of $E=67.5$ GPa, Poisson coefficient of $\upsilon=0.35$, and density of $\rho=2700$ kg m^{-3}. A yield stress of 800 MPa was used. The simulations were performed with a displacement velocity of 10 mm min^{-1} without friction. Isothermal condition was assumed, which can be justified by the low velocity. The simulations were carried out for the $p/c=2$ NECAP geometry.

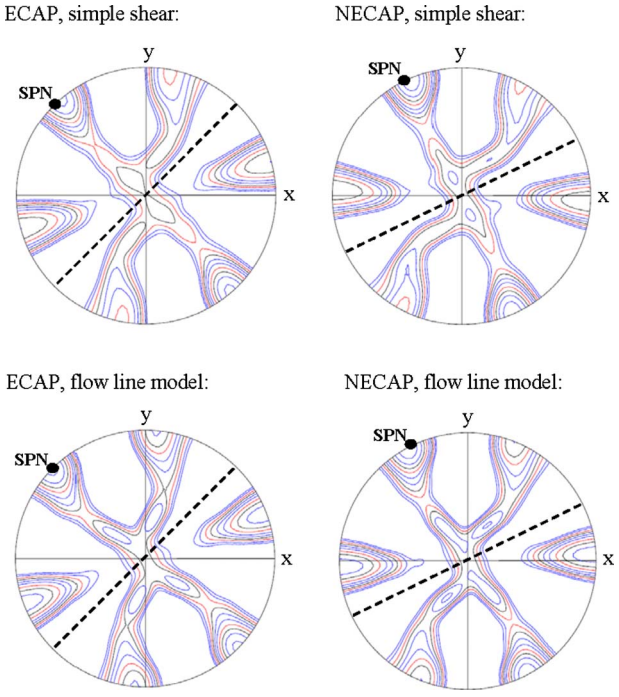

Fig. 6 {111} pole figures showing the textures after one pass in ECAP and in NECAP ($p/c=2$). The dotted lines indicate the ideal shear plane and SPN is the shear plane normal. Isovalues: 0.8, 1, 1.3, 1.6, 2, 2.5, 3.2, 4, 5, and 6.4.

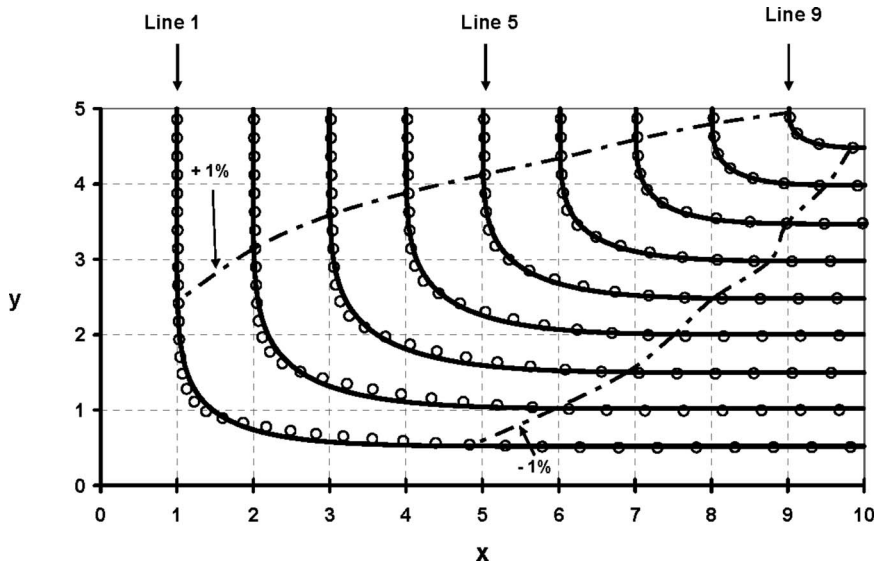

Fig. 7 Flow lines obtained from finite element analysis (identified by circles) and fitted by the proposed flow line function (continuous lines) in NECAP ($p/c=2$). The broken lines indicate the extent of the strain zone, where +1% means 1% of the total strain and −1% is 99% of the total strain in one pass.

The obtained trajectory lines are shown in Fig. 7 (identified by circles). Ten lines were selected; for each of them the proposed flow line function was fitted to obtain the n parameter, which is the only parameter of the flow line. As can be seen in Fig. 7, the trajectories can be well approximated by the analytic flow function (continuous lines). Only the n parameter changes from one line to the other (together with the entering position x_0 of the line). Its variation as a function of x_0 is shown in Fig. 8; n decreases within the plastic zone from the outer corner to the inner corner. Similar kind of variations of the n exponent in the case of ECAP has already been reported before [15,27–29]. Although this dependence of n on x_0 was neglected in the mathematical treatment of the problem in Sec. 3 above, the results of calculations (not shown here) where n is considered to be variable indicated that the resulting velocity field was very slightly affected by this variation [30]. Similar results are expected for the present NECAP case and will be studied in future works. Figure 8 shows also the total strain accumulated in one pass as a function of the entering position of the flow line within the die. The predicted variation is quite significant; it decreases with x_0.

Figure 7 also shows the extent of the plastic zone within the NECAP die. The two broken lines identified with +1% and −1% show the entering and finishing points of the plastic zone. In theory, there is plastic strain everywhere along the proposed flow line, in practice; however, the strains are extremely small at the initial and finishing parts of the flow lines before and after the plastic zone, respectively. The strain of 1% with respect to the total strain in one pass was selected to detect the beginning of the plastic zone and 1% less than the total strain to locate the end of the plastic zone. As can be seen in Fig. 7, the plastic zone is quite large around the intersection plane of the channels and has a fan shape.

An important parameter of the deformation process is the strain rate. Figure 9 displays the strain rate variations within the plastic

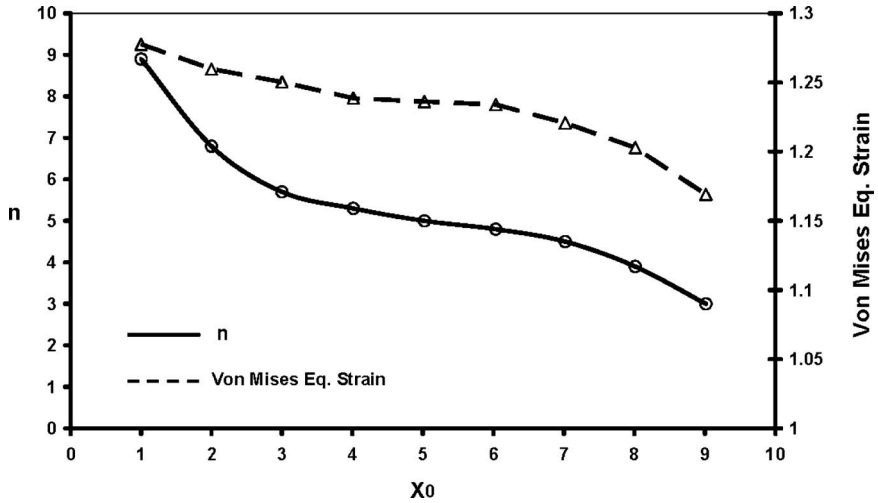

Fig. 8 The n parameter of the flow line and the accumulated von Mises strain in one pass as a function of its entering position x_0 within the NECAP die as it is obtained from fitting of the FE-obtained trajectories.

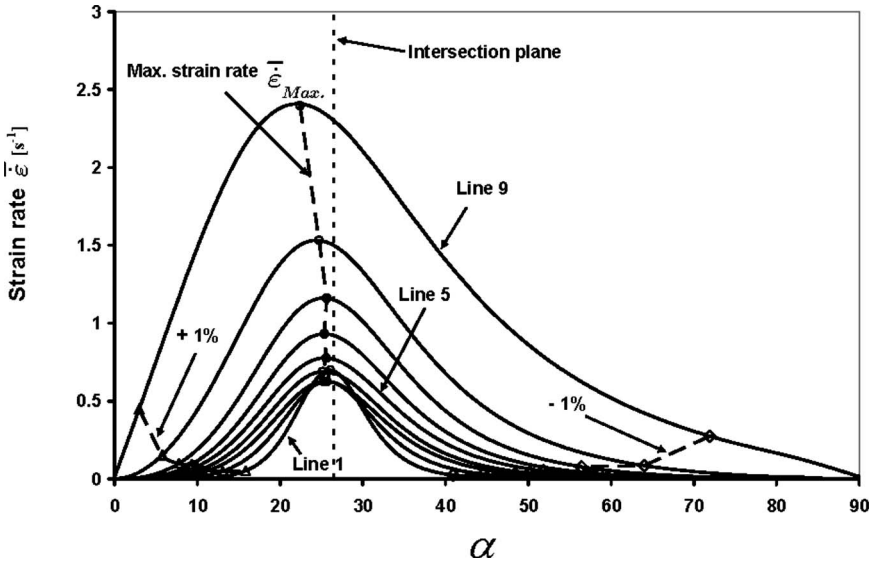

Fig. 9 Variation of the von Mises equivalent strain rate along the flow lines as a function of the angular position (obtained from the flow line approach). The punch velocity is 10 mm/min, and the die thickness is p/c=10 mm/5 mm

zone that was identified in Fig. 7. As expected, the strain rate is larger at the inner corner and decreases toward the outer corner. It can be also seen in Fig. 9 that the location of the maximum value along a given line does not coincide with the position of the intersection plane in general; it occurs before the theoretical shear plane is attained.

From the above analysis, we can conclude that good agreements are obtained between the finite-element-predicted and analytic flow lines that represent a good validation of the proposed flow line function.

6 Concluding Remarks

A modification to the existing ECAP process is proposed in the present work that consists in decreasing the diameter of the outgoing channel; the process is named NECAP. An analysis of the deformation mode was carried out for such a die, for the case when the angle of the channels is 90 deg. It has been shown that the process remains simple shear in the ideal conditions where the shear plane is the intersection plane of the channels. An analytic formula was derived to obtain the total shear in one pass, which agrees with the formula derived by Lee [6]. Then a flow function was proposed to describe the strain mode in a continuous way. Comparisons between the deformation modes for ECAP and NECAP were carried out. The flow function was also validated by finite element calculations. One of the main interests of the present work was to derive the deformation mode, which permitted to predict the evolution of the crystallographic texture during extrusion. Simulations were carried out using the viscoplastic self-consistent polycrystal code to obtain the characteristics of the textures that can develop in NECAP of fcc materials.

One of the main features of the deformation mode in NECAP is that the shear plane approaches more the plane of the process, that is, the ND (normal direction) plane. In this way, the shear textures that develop are such that the {111} ideal fiber plane is nearer to the ND plane. Such textures are sought for their higher formability in sheet forming for aluminum sheets. Therefore, the NECAP process could be used before conventional rolling to improve the initial texture from which the final rolling texture is obtained. Also, sheets could be directly deformed by NECAP to obtain improved textures although no specific recommendations could be forwarded in the present article to solve the technical problems in industrial applications. That could be the subject of future research.

Although the inclination of the texture is different in NECAP and it can influence macroscopic properties, the texture itself is nearly the same as in ECAP when rotated into a common reference system. This means that if texture has an effect on the grain refinement process (which has not yet confirmed in the literature), no significant differences in grain fragmentation are expected only from the texture.

Another important aspect of the NECAP process is related to the hydrostatic pressure. The application of a back pressure, developed by Lapovok [5], showed to be very efficient in the stability of the ECAP process. By reducing the diameter of the outgoing channel, such back pressure develops automatically in NECAP.

Finally, it is probable that the grain fragmentation process is faster in NECAP compared with ECAP, which can make NECAP a more effective process for obtaining bulk nanostructured materials. The following arguments can be forwarded to support this hypothesis: (1) The strain is larger in one pass by about 25% (for a reduction ratio of 50%). (2) Much larger hydrostatic stresses are present compared with ECAP, which are also contributing to the grain refinement process. Examples are the ECAP with back pressure [5] and high pressure torsion test [31], where the grain size is smaller at equivalent strain compared with tests without hydrostatic stresses. (3) There is much more elongation in the grain shape in NECAP than in ECAP, which also helps grain subdivision through the geometrical process proposed by Gholinia et al. [32].

References

[1] Segal, V. M., 1974, Ph.D. thesis, Minsk, Russia.
[2] Segal, V. M., Reznikov, V. I., Drobyshevkiy, A. E., and Kopylov, V. I., 1981, "Plastic Working of Metals by Simple Shear," Russ. Metall. **1**, pp. 99–105.
[3] Segal, V. M., 1982, "Thermomechanical Treatment of the Elinvar Alloy 44NKhMT Using Plain Shear," Metal Sci. Heat Treat., **24**, pp. 706–710.
[4] Valiev, R. Z., and Langdon, T. G., 2006, "Principles of Equal-Channel Angular Pressing as a Processing Tool for Grain Refinement," Prog. Mater. Sci., **51**, pp. 881–981.
[5] Lapovok, R., 2005, "The Role of Back-Pressure in Equal Channel Angular Extrusion," J. Mater. Sci., **40**, pp. 341–346.
[6] Lee, D. N., 2000, "An Upper-Bound Solution of Channel Angular Deformation," Scr. Mater., **43**, pp. 115–118.
[7] Lee, J. C., Seok, H. K., Han, J. H., and Chung, Y. H., 2001, "Controlling the Textures of the Metal Strips via the Continuous Confined Strip Shearing (C2S2) Process," Mater. Res. Bull., **36**, pp. 997–1004.
[8] Lee, J. C., Seok, H. K., and Suh, J. Y., 2002, "Microstructural Evolutions of the Al Strip Prepared by Cold Rolling and Continuous Equal Channel Angular Pressing," Acta Mater., **50**, pp. 4005–4019.

[9] Han, J. H., Oh, K. H., and Lee, J. C., 2003, "Effect of Initial Texture on Texture Evolution in 1050 Al Alloys Under Simple Shear," Metall. Mater. Trans. A, **34**, pp. 1675–1681.
[10] Lee, J. C., Suh, J. Y., and Ahn, J. P., 2003, "Work-Softening Behavior of the Ultrafine-Grained Al Alloy Processed by High-Strain-Rate, Dissimilar-Channel Angular Pressing," Metall. Mater. Trans. A, **34**, pp. 625–632.
[11] Han, J. H., Suhb, J. Y., Jee, K. K., and Lee, J. C., 2008, "Evaluation of Formability and Planar Anisotropy Based on Textures in Aluminum Alloys Processed by a Shear Deforming Process," Mater. Sci. Eng., A, **477**, pp. 107–120.
[12] Segal, V. M., 1999, "Equal Channel Angular Extrusion: From Macromechanics to Structure Formation," Mater. Sci. Eng., A, **271**, pp. 322–333.
[13] Han, W. Z., Zhang, Z. F., Wu, S. D., and Li, S. X., 2007, "Influences of Crystallographic Orientations on Deformation Mechanism and Grain Refinement of Al Single Crystals Subjected to One-Pass Equal-Channel Angular Pressing," Acta Mater., **55**, pp. 5889–5900.
[14] Iwahashi, Y., Wang, J., Horita, Z., Nemoto, M., and Langdon, T. G., 1996, "Principle of Equal-Channel Angular Pressing for the Processing of Ultra-Fine Grained Materials," Scr. Mater., **35**, pp. 143–146.
[15] Tóth, L. S., Arruffat-Massion, R., Baik, S. C., Germain, L., and Suwas, S., 2004, "Analysis of Texture Evolution in Equal Channel Angular Extrusion of Copper Using a New Flow Field," Acta Mater., **52**, pp. 1885–1898.
[16] Zisman, A. A., Rybin, V. V., Van Boxel, S., Seefeldt, M., and Verlinden, M. B., 2006, "Equal Channel Angular Drawing of Aluminium Sheet," Mater. Sci. Eng., A, **427**, pp. 123–129.
[17] Jin, Y. H., Huh, M. Y., and Chung, Y. H., 2004, "Evolution of Textures and Microstructures in IF-Steel Sheets During Continuous Confined Strip Shearing and Subsequent Recrystallization Annealing," J. Mater. Sci., **39**, pp. 5311–5314.
[18] Huang, Y., and Prangnell, P. B., 2007, "Continuous Frictional Angular Extrusion and Its Application in the Production of Ultrafine-Grained Sheet Metals," Scr. Mater., **56**, pp. 333–336.
[19] Lapovok, R., McKenzie, P. W. J., Thomson, P. F., and Semiatin, S. L., 2007, "Processing and Properties of Ultrafine-Grain Aluminum Alloy 5005 Sheet," J. Mater. Sci., **42**, pp. 1649–1659.
[20] Saito, Y., Utsunomiya, H., Tsuji, N., and Sakai, T., 1999, "Novel Ultra-High Straining Process for Bulk Materials—Development of the Accumulative Roll-Bonding (ARB) Process," Acta Mater., **47**, pp. 579–583.
[21] Hasani, A., and Tóth, L. S., 2009, "A Fan-Type Flow-Line Model in Equal Channel Angular Extrusion," Scr. Mater., **61**, pp. 24–27.
[22] Altan, S. B., Antar, N., and Gultekin, E., 1992, "A Comparison of Some Deformation Models in Axisymmetric Extrusion," J. Mater. Process. Technol., **33**, pp. 263–272.
[23] Beyerlein, I. J., and Tóth, L. S., 2009, "Texture Evolution in Equal-Channel Angular Extrusion," Prog. Mater. Sci., **54**, pp. 427–510.
[24] Molinari, A., and Tóth, L. S., 1994, "Tuning a Self Consistent Viscoplastic Model by Finite Element Results—I. Modeling," Acta Metall. Mater., **42**, pp. 2453–2458.
[25] Beyerlein, I. J., Li, S., Necker, C. T., Alexander, D. J., and Tomé, C. N., 2005, "Non-Uniform Microstructure and Texture Evolution During Equal Channel Angular Extrusion," Philos. Mag., **85**, pp. 1359–1394.
[26] Zaïri, F., Aour, B., Gloaguen, J. M., Naït-Abdelaziz, M., and Lefebvre, J. M., 2006, "Numerical Modelling of Elastic-Viscoplastic Equal Channel Angular Extrusion Process of a Polymer," Comput. Mater. Sci., **38**, pp. 202–216.
[27] Skrotzki, W., Scheerbaum, N., Oertel, C. G., Arruffat-Massion, R., Suwas, S., and Tóth, L. S., 2007, "Microstructure and Texture Gradient in Copper Deformed by Equal Channel Angular Pressing," Acta Mater., **55**, pp. 2013–2024.
[28] Skrotzki, W., Tóth, L. S., Klöden, B., Brokmeier, H. G., and Arruffat-Massion, R., 2008, "Texture After ECAP of a Cube-Oriented Ni Single Crystal," Acta Mater., **56**, pp. 3439–3449.
[29] Hasani, A., Lapovok, R., Tóth, L. S., and Molinari, A., 2008, "Deformation Field Variations in Equal Channel Angular Extrusion Due to Back Pressure," Scr. Mater., **58**, pp. 771–774.
[30] Hasani, A., 2009, Ph.D. thesis, University of Metz, France.
[31] Zhilyaev, A. P., McNelley, T. R., and Langdon, T. G., 2007, "Evolution of Microstructure and Microtexture in fcc Metals During High-Pressure Torsion," J. Mater. Sci., **42**, pp. 1517–1528.
[32] Gholinia, A., Prangnell, P. B., and Markushev, M. V., 2000, "The Effect of Strain Path on the Development of Deformation Structures in Severely Deformed Aluminium Alloys Processed by ECAE," Acta Mater., **48**, pp. 1115–1130.